Design, Fabrication, and Control of Components in MEMS-Based Optical Pickups

Yi Chiu[1], Jin-Chern Chiou[1], Weileun Fang[2], Yung-Jiun Lin[1], and Mingching Wu[2]

[1]Department of Electrical and Control Engineering, National Chiao Tung University, Hsin Chu, Taiwan, R.O.C.
[2]Department of Power Mechanical Engineering, National Tsing Hwa University, Hsin Chu, Taiwan, R.O.C.

Small-form-factor optical pickups and disk drives have been an area of intense research since the rise of portable consumer electronic products. In current technology, most of the devices are manufactured by the precision assembly of discrete miniaturized optomechanical components. The assembly process can be simplified and cost reduced by using the batch fabrication processes developed in microelectromechanical systems (MEMS). In this paper, the fabrication and testing of optical and actuator components for a MEMS-based optical pickup are presented. A novel design methodology is also applied to the servo control system of the pickup.

Index Terms—**Actuator, microelectromechanical systems (MEMS), optical pickup, silicon on insulation (SOI), small form factor.**

I. INTRODUCTION

AS the blue optical storage technology matures, other storage mechanisms such as hologram, near field, and multi layer/level are being eagerly pursued. From the application point of view, microdisk drives for portable consumer devices, such as mobile phones and portable media players, are also an area of intense research. In this regard, small-form-factor optical drive and pickup technologies have been proposed or commercialized. In [1], the drive was constructed by the assembly of miniaturized optomechanical components found in conventional drives. In [2] and [3], a miniaturized optical pickup unit containing the laser diode (LD), photodetectors (PD), and optical components was assembled and mounted in a swing arm actuator. In [4]–[6], similar optical pickup modules were used in a more traditional head assembly or testbed. In [7], a slider-type optical flying head and a separate base optical unit containing LD, PD, and optical components were assembled on a swing arm actuator. In these works, most of the microoptical, mechanical (actuator), and electrical (LD and PD) components are conventional discrete components. The assembly of numerous microparts becomes tedious and the cost of the system can not be reduced easily.

To reduce the number of components, several approaches based on some forms of semiconductor fabrication processes have been proposed. However, the planar integrated optics approach suffers from high coupling and waveguide losses [8]. Stacking of planar optical components is challenged in the alignment and assembly processes [9]. In [10], a microoptical pickup based on the microelectromechanical systems (MEMS) technology was proposed. It then becomes possible to integrate optical, mechanical, and electrical components all in a common

substrate. In [11], we proposed such a MEMS-based optical pickup composed of an electrooptical and an actuator chips, both of which are fabricated monolithically. The assembly process can, therefore, be much simplified. In this paper, we present the design, fabrication, and control of the components in this MEMS-based optical pickup.

II. ELECTROOPTICAL CHIP

Surface micromachining is an important technology in MEMS due to its design versatility and IC-like fabrication. It has gained another degree of freedom in the vertical dimension since the demonstration of microhinges and microoptical benches [12], [13]. Traditional surface micromachining uses thin poly-silicon layers as the structural and optical material. However, it has several disadvantages for optical applications, such as surface curvature induced by residual stress, absorption of visible light, and poor performance as an optical detector. To increase the stiffness and reduce the effect of residual stress, structures employing high-aspect-ratio poly-silicon processes or silicon-on-insulation (SOI) wafers were proposed [14]–[16]. However, the high deposition temperature of poly-silicon in these processes may affect the performance of photo detectors or circuits if they are to be fabricated on the same substrate. In this paper, a novel fabrication process to integrate SOI and SU-8 negative photoresist is demonstrated as a low-temperature and inexpensive process compared to the current technologies. In this process, signal processing circuits, photo detectors, and flat mirror surfaces are fabricated in the SOI device layer; microoptical devices and stressed related structures can be fabricated in the SU-8 layer.

As an example, the fabrication process of a flipped mirror is shown in Fig. 1. The micromirror structure is first defined in the device layer of the SOI substrate using deep reactive ion etching (DRIE), followed by the fabrication of circuits and photo diodes [Fig. 1(a)]. An oxide layer is then deposited and patterned as the second sacrificial layer [Fig. 1(b)]. Gold is deposited and patterned for electrical contact and mirror surface. Finally, SU-8 is spin-coated and patterned. The structures are then released
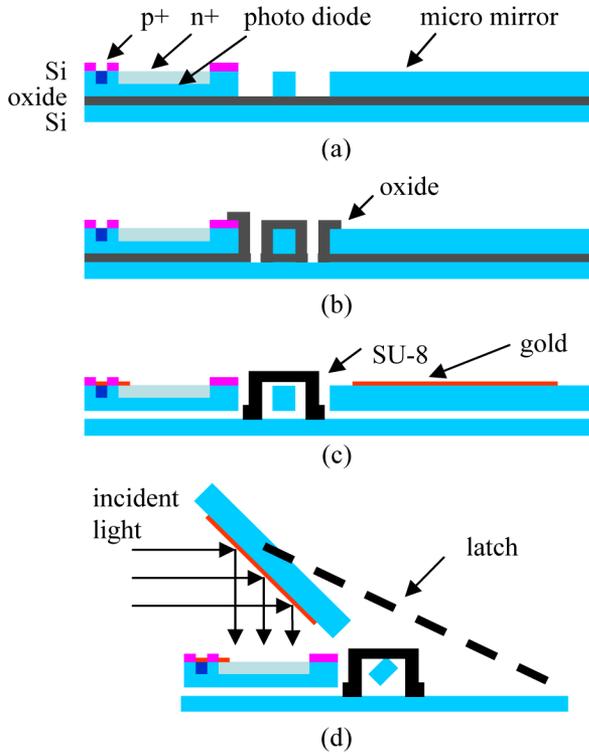
Fig. 1. Fabrication processes of the electrooptical chip. (a) Define structure and fabricate photodiode. (b) Deposit and define oxide sacrificial layer. (c) Deposit and define gold; spin-coat and define SU-8; release. (d) Flip and assemble mirror.

Fig. 2. Fabricated micromirror and photo diode.
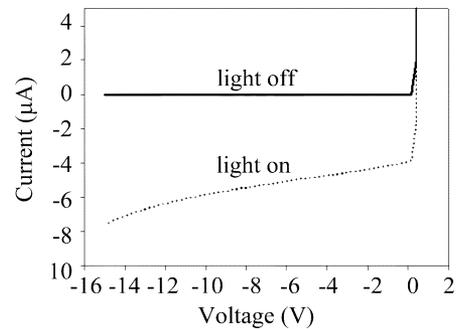
Fig. 3. I–V curves of the photo diode.
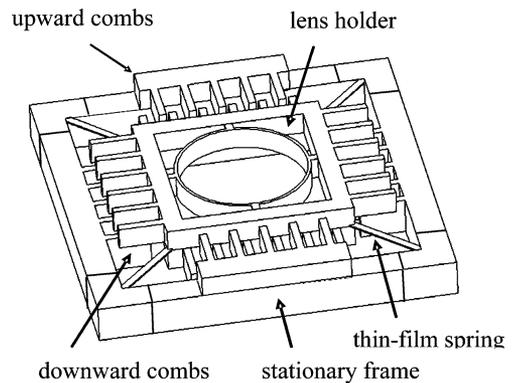
Fig. 4. Schematic of the bidirectional focusing actuator.

by HF etching [Fig. 1(c)]. Due to the residual stress developed in SU-8, SU-8/Si bimorph beams can be used as lifting arms to facilitate microassembly. Optical devices such as gratings or Fresnel lens can be patterned in the SU-8 layer which has high transmittance in the visible spectrum range. Fig. 1(d) shows the schematic of a 135°-flipped mirror with an underneath photo diode to detect the returned optical signal from the disc.

Fig. 2 is a micromirror fabricated using this process before flipping, showing the flat single-crystal-silicon mirror surface, SU-8 hinges, stressed beams, and photo diodes. The measured residual stress in SU-8 is about 27 MPa, close to that reported in the literature [17]. The I–V curves of the photo diodes are shown in Fig. 3. The measured sensitivity is about 1.8 A/W at 650-nm wavelength. Therefore, the simple and inexpensive fabrication process is demonstrated for the integration of microoptical devices and photo detectors. Our current efforts are focused on better mechanism design and integration of other optical components in the pickup.

III. SERVO ACTUATOR

A. Design Concept

Piezoelectric actuators [18] and bimorph thermal actuators [19] have been exploited as tracking servo actuators in data storage systems. Electrostatic optical focusing actuators have also been demonstrated in [20]. However, it is difficult to integrate the actuator component and the objective lens mono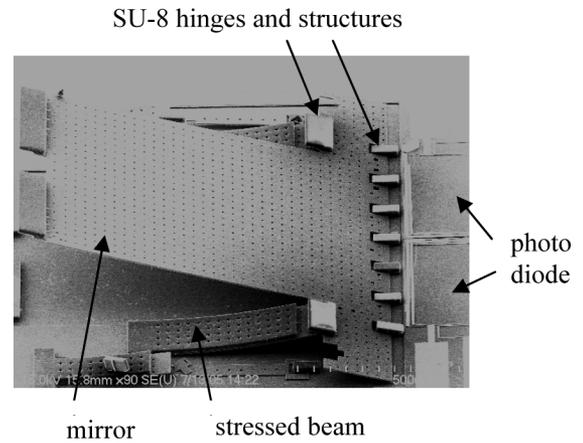lithically on a single chip. It this paper, we demonstrate a novel bidirectional focusing actuator and integrated UV-cured polymer lens on a single chip using self-aligned vertical comb drive structure.

The schematic of the out-of-plane bidirectional focusing actuator is shown in Fig. 4. It is composed of vertical comb actuators, a lens holder, and a UV-cured polymer lens (or a microball lens). The movable lens holder is connected to a stationary rigid frame by four thin-film springs. The upward or downward position of the lens holder is controlled by two sets of vertical comb actuators. As indicated in Fig. 4, the moving electrodes are located below the stationary electrodes in the upward actuator, whereas the moving electrodes are above the stationary electrodes in the downward actuator. The stationary electrodes

of the upward and the downward actuators are electrically isolated and can be individually actuated; the moving electrodes are grounded through thin-film springs.

The thickness and location of the vertical comb electrodes can be controlled by the process to improve the traveling distance and driving voltage [21]. In the current design, the thickness of movable combs and stationary combs are both 20 μm so that the expected maximum traveling distance is 20 μm. However, the travel distance could be limited by the side-sticking effect due to the misalignment of the comb electrodes [22]. This issue is addressed by the self-aligned fabrication process [23]. The width and thickness of the thin-film springs are 20 and 2 μm, respectively. Therefore, the ratio between the in-plane and the out-of-plane stiffness is close to 100, which also helps suppress the side-sticking effect.

B. Fabrication and Testing

The fabrication processes of this actuator are illustrated in Fig. 5. It begins with the growth and patterning of thermal oxide [Fig. 5(a)]. A second photolithography is used to define the self-aligned trench structure. The photoresist in Fig. 5(a) is removed after the first DRIE. The thermal oxide is then used as the etching mask of the second DRIE. The self-aligned trenches with two different depths after the second DRIE are shown in Fig. 5(b). After that, the trenches are fully refilled with thermal oxide and poly-silicon (Poly1) deposited by low pressure chemical vapor deposition (LPCVD) [Fig. 5(c)]. After Poly1 is patterned, a Si_xN_y layer and the second poly-silicon (Poly2) layer are deposited and patterned for structures and electrical interconnection [Fig. 5(d)]. The third DRIE is used to etch Poly1 again to define the vertical comb structures [Fig. 5(d)]. In addition, the lens holder is implemented in the shallow refilled trenches. In Fig. 5(e), low stress nitride is deposited and patterned as the mask for the subsequent bulk silicon etching. The substrate is then etched in the tetramethyl ammonium hydroxide (TMAH) solution to release the suspended poly-silicon structure which is fully protected by the thermal oxide and Si_xN_y films. A through hole is fabricated for light to pass through the wafer. Finally, the protection layers are removed and a UV-curable polymer droplet is dropped to the lens holder, as shown in Fig. 5(f).

Fig. 6(a) shows the fabricated actuator. The initial engagement between the upward and downward combs is 3 μm to provide a large electrostatic driving force. Fig. 6(b) shows the UV-cured polymer lens centered in the lens holder with a diameter of 200 μm. The measured surface roughness of the lens is smaller than 5 nm. The focusing of light by the polymer lens can be observed on a CCD monitor. The typical spot size is 5 μm and the numerical aperture is 0.3. Whereas the polymer lens is used to demonstrate the functionality of the integrated module, a dedicated molded lens may be mounted to the lens holder for practical application. The static and dynamic out-of-plane displacements of the actuator are shown in Fig. 7. The maximum static displacements for both upward and downward directions are 12.5 μm for a driving voltage of 35 V. The dynamic response shows a resonant frequency of the first out-of-plane spring bending mode of 1.1 kHz. Therefore, an out-of-plane
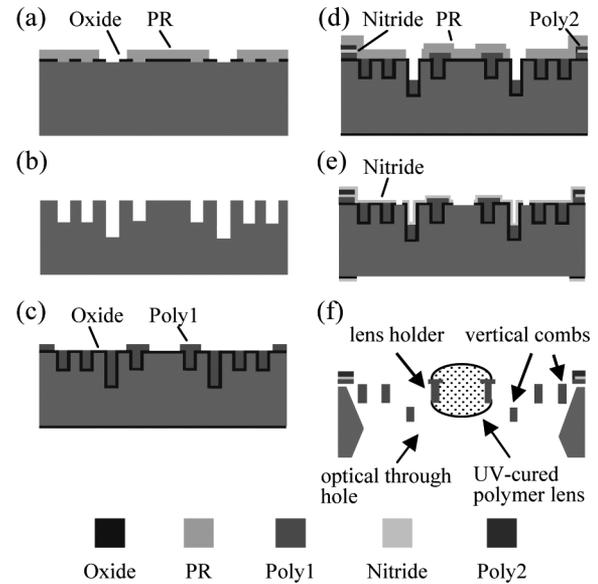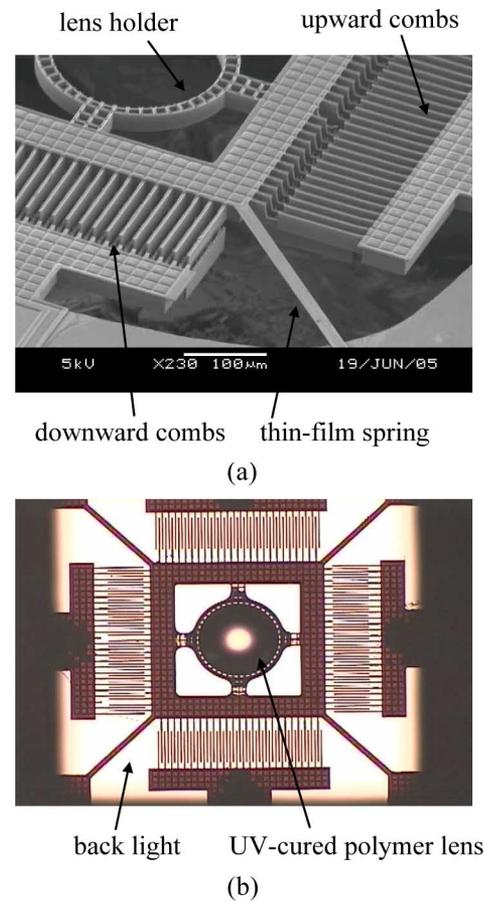

Fig. 5. Fabrication processes of the actuator.

Fig. 6. Fabricated focusing actuator.

bidirectional focusing MEMS actuator with a large bandwidth is demonstrated. Our current efforts are focused on the integration of focusing and tracking actuators using the same fabrication platform.
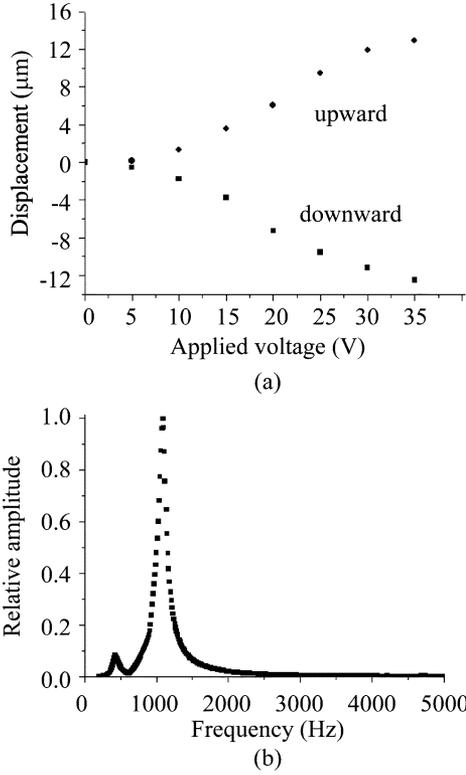
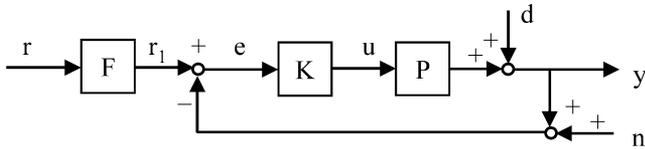Fig. 7.   (a) Static and (b) dynamic responses of the actuator.

Fig. 8.   Two-degree-of-freedom uncertain feedback system.

IV. Servo Control

Traditional servo control design in optical disk drives employs PID or lead-lag compensation and trial-and-error procedures to find the optimal controller parameters. While simple in principle, it is less efficient and more susceptible to the variation of component characteristics. Therefore, a more systematic and roubust approach combining the quantitative feedback theory (QFT) and the H_∞ theory [24] is demonstrated for the servo control design in optical disk drives. In this approach, the H_∞ theory improves the complicated Nichol charts in the QFT design. On the other hand, the QFT is used to find the weighting functions in the H_∞ control theory.

A two-degree-of-freedom uncertain feedback system is used to model the pickup servo system where P is the plant, K is the controller, and F is a prefilter used to adjust the system characteristics (Fig. 8). The QFT/H_∞ design approach consists of two stages. In the first stage, the system characteristics in the time domain, such as settling time and overshoot, are translated as the upper and lower allowable bounds in the frequency domain. The controller parameters are then found by using the combined design technique. In the second stage, the prefilter outside the control loop is used to achieve the system specifications as practiced
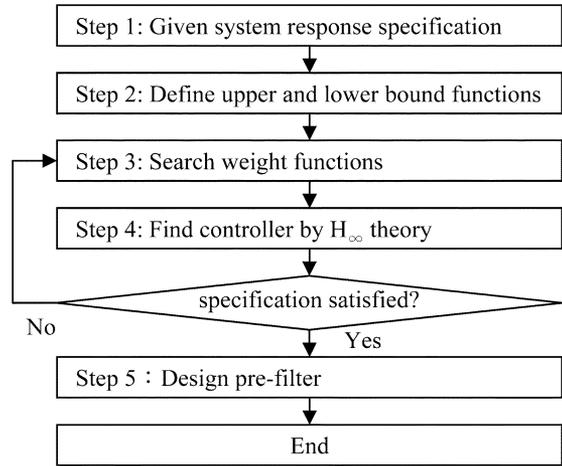

Fig. 9.   QFT/H_∞ design flow.

in the QFT design procedure. The overall design flow is illustrated in Fig. 9.

The tracking servo in a commercial DVD ROM drive is used to demonstrate the combined QFT/H_∞ design approach. The transfer function of the tracking actuator is given as

$$P(s) = \frac{30000}{s^2 + 6.883s + 30000}$$

and the time domain sepcifications of the tracking system are

$$\text{settling time}: t_s \leq 0.002 \text{ s}$$
$$\text{maximum overshoot}: M_p \leq 10\%.$$

The time domain specifications [Fig. 10(a)] are translated to the upper and lower bounds in the frequency domain [Fig. 10(b)]. The controller K and prefilter F are then obtained by the QFT/H_∞ design approach as

$$K(s) = \frac{20265.7453(s + 965.8)(s^2 + 6.883s + 30000)}{(s + 5)^2(s^2 + 2.711 \times 10^4 s + 3.668 \times 10^8)}$$
$$F(s) = \frac{200000}{(s + 200)(s + 1000)}.$$

The closed loop responses in both time and frequency domains are shown in Fig. 10 to be within the system specification.

The controller and prefilter are programmed into the firmware of a commercial DVD ROM drive. Fig. 11 shows the improved tracking error signal of a track jump operation using the new controller as compared to that obtained by using the default controller. Therefore, the robust control design based on QFT/H_∞ and its application to the optical drive design is successfully demonstrated.

V. Conclusion

Novel electrooptical modules, microactuators, and control system design methodology for a MEMS-based micropickup are proposed and demonstrated. The new fabrication processes of the microoptical bench provide a platform for the integration of circuits, photo detectors and optical components. The microactuator with UV cured polymer lens shows the capability of focusing control. The more systematic QFT/H_∞ design approach has been verified in a traditional optical pickup. Our
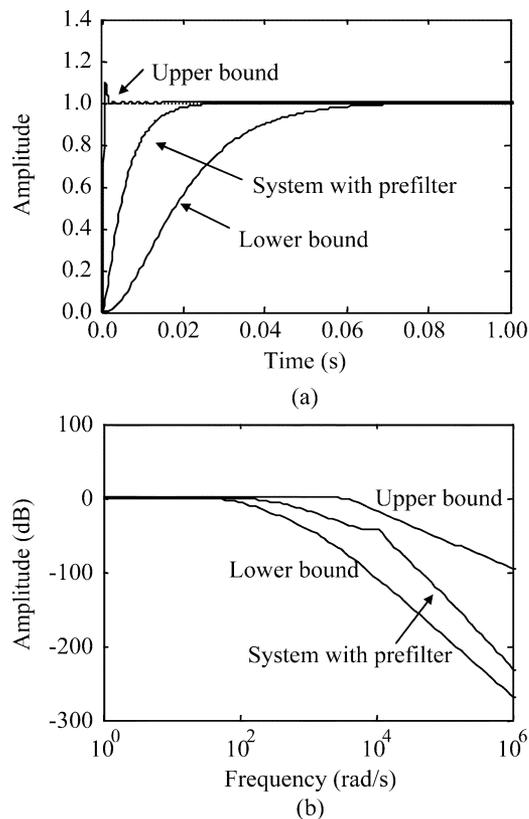
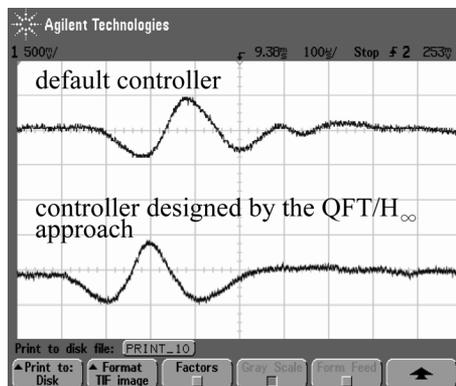Fig. 10. Tracing servo response (a) time domain and (b) frequency domain.

Fig. 11. Tracking error signal.

current efforts are focused on the two-chip packaging process for the electrooptical and actuator chips. The microactuators are also being characterized in the combined QFT/H$_\infty$ servo system design flow.

ACKNOWLEDGMENT

REFERENCES

[1] M. A. H. van der Aa, *et al.*, "Highly miniaturised prototype optical drive for use in portable devices," *Proc. SPIE*, vol. 5069, pp. 1–4, 2003.
[2] D. L. Blankenbeckler, B. W. Bell, Jr., K. Ramadurai, and R. L. Mahajan, "Recent advancements in DataPlay's small form-factor optical disc and drive," *Jpn. J. Appl. Phys.*, vol. 45, no. 2B, pp. 1181–1186, 2006.
[3] J. S. Sohn, *et al.*, "Development of integrated optical pickup for small form factor optical disc drive," *Proc. SPIE*, vol. 6282, pp. 10–16, 2006.
[4] K. Manoh, *et al.*, "Small integrated optical head device using a blue-violet laser diode for Blu-ray disc dystem," *Jpn. J. Appl. Phys.*, vol. 42, no. 2B, pp. 880–884, 2003.
[5] M. Horiyama, *et al.*, "Optical pickup using integrated optical unit for Blu-ray disc," *Proc. SPIE*, vol. 6282, pp. 41–48, 2006.
[6] H. F. Shih, C. L. Chang, K. J. Lee, and C. S. Chang, "Design of optical head with holographic optical element for small form factor drive systems," *IEEE Trans. Magn.*, vol. 41, no. 2, pp. 1058–1060, Feb. 2005.
[7] S. Kim, *et al.*, "An optical flying head assembly for a small-form-factor plastic disk in PCMCIA-like drive," *Jpn. J. Appl. Phys.*, vol. 43, no. 7B, pp. 4752–4758, 2004.
[8] S. Ura, T. Suhara, H. Nishihara, and J. Koyama, "An integrated-optic disc pickup device," in *Proc. Electronics Communications in Japan, Part 2: Electronics*, 1987, vol. 70, no. 2, pp. 92–100.
[9] J. Y. Chang, C. M. Wang, C. C. Lee, H. F. Shih, and M. L. Wu, "Realization of free-space optical pickup head with stacked Si-based phase elements," *IEEE Photon. Technol. Lett.*, vol. 17, no. 1, pp. 214–216, Jan. 2005.
[10] M. Wu, "Micromachining for optical and optoelectronic systems," *Proc. IEEE*, vol. 85, no. 11, pp. 1833–1856, Nov. 1997.
[11] Y. Chiu, C. H. Chen, J. C. Chiou, W. Fang, and H. P. D. Shieh, "MEMS-based miniature optical pickup," *IEEE Trans. Magn.*, vol. 41, no. 2, pp. 967–970, Feb. 2005.
[12] K. S. J. Pister, M. W. Judy, S. R. Burgett, and R. S. Fearing, "Microfabricated hinges," *Sens. Actuators A*, vol. 33, no. 3, pp. 249–256, 1992.
[13] M. C. Wu, L. Y. Lin, S. S. Lee, and K. S. J. Pister, "Micromachined free-space integrated micro-optics," *Sens. Actuators A*, vol. 50, no. 1–2, pp. 127–134, 1995.
[14] C. G. Keller and R. T. Howe, "Hexsil tweezers for teleoperated microassembly," in *Proc. Dig. IEEE MEMS*, 1997, pp. 72–77.
[15] F. Ayazi and K. Najafi, "High aspect-ratio combined poly and single-crystal silicon (HARPSS) MEMS technology," *J. Microelectromech. Syst.*, vol. 9, pp. 288–294, 2000.
[16] V. Milanovic, "Multilevel-beam SOI-MEMS fabrication and applications," *J. Microelectromech. Syst.*, vol. 13, no. 1, pp. 19–30, 2004.
[17] R. Feng and R. J. Farris, "Influence of processing conditions on the thermal and mechanical properties of SU8 negative photoresist coatings," *J. Micromech. Microeng.*, vol. 13, no. 1, pp. 80–88, 2003.
[18] Y. Yee, H. J. Nam, S. H. Lee, J. U. Bu, Y. S. Jeon, and S. M. Cho, "PZT actuated micromirror for nano-tracking of laser beam for high-density optical data storage," in *Proc. Dig. IEEE MEMS*, 2000, pp. 435–438.
[19] J. P. Yang, X. C. Deng, and T. C. Chong, "An electro-thermal bimorph-based microactuator for precise track-positioning of optical disk drives," *J. Micromech. Microeng.*, vol. 15, no. 5, pp. 958–965, 2005.
[20] S. H. Kim, *et al.*, "Integrated micro optical flying head with lens positioning actuator for small form factor data storage," in *Proc. Dig. Int. Conf. Solid-State Sensors, Actuators, Microsystems (Tranducers)*, 2003, pp. 607–610.
[21] J. M. L. Tsai, H. Y. Chu, J. Hsieh, and W. Fang, "The BELST II process for silicon HARM vertical comb actuator and its applications," *J. Micromech. Microeng.*, vol. 14, no. 2, pp. 235–241, 2004.
[22] O. Tsuboi, *et al.*, "Rotational comb-driven micromirror with a large deflection angle and low drive voltage," in *Proc. Dig. IEEE MEMS*, 2002, pp. 532–535.
[23] M. Wu and W. Fang, "Design and fabrication of MEMS devices using the integration of MUMPs, trench-refilled molding, DRIE and bulk silicon etching processes," *J. Micromech. Microeng.*, vol. 15, no. 3, pp. 535–42, 2005.
[24] M. J. Sidi, "A combined QFT/H$_\infty$ design technique for TDOF uncertain feedback systems," *Int. J. Control*, vol. 75, no. 7, pp. 475–489, 2002.